ORIGINAL ARTICLE

Climatic water deficit, tree species ranges, and climate change in Yosemite National Park

James A. Lutz[1]*, Jan W. van Wagtendonk[2] and Jerry F. Franklin[1]

[1]*College of the Environment, University of Washington, Box 352100, Seattle, WA 98195-2100, USA,* [2]*US Geological Survey, Western Ecological Research Center, Yosemite Field Station, 5083 Foresta Road, El Portal, CA 95318-0700, USA*

ABSTRACT

Aim (1) To calculate annual potential evapotranspiration (PET), actual evapotranspiration (AET) and climatic water deficit (Deficit) with high spatial resolution; (2) to describe distributions for 17 tree species over a 2300-m elevation gradient in a 3000-km² landscape relative to AET and Deficit; (3) to examine changes in AET and Deficit between past (*c.* 1700), present (1971–2000) and future (2020–49) climatological means derived from proxies, observations and projections; and (4) to infer how the magnitude of changing Deficit may contribute to changes in forest structure and composition.

Location Yosemite National Park, California, USA.

Methods We calculated the water balance within Yosemite National Park using a modified Thornthwaite-type method and correlated AET and Deficit with tree species distribution. We used input data sets with different spatial resolutions parameterized for variation in latitude, precipitation, temperature, soil water-holding capacity, slope and aspect. We used climate proxies and climate projections to model AET and Deficit for past and future climate. We compared the modelled future water balance in Yosemite with current species water-balance ranges in North America.

Results We calculated species climatic envelopes over broad ranges of environmental gradients – a range of 310 mm for soil water-holding capacity, 48.3°C for mean monthly temperature (January minima to July maxima), and 918 mm yr⁻¹ for annual precipitation. Tree species means were differentiated by AET and Deficit, and at higher levels of Deficit, species means were increasingly differentiated. Modelled Deficit for all species increased by a mean of 5% between past (*c.* 1700) and present (1971–2000). Projected increases in Deficit between present and future (2020–49) were 23% across all plots.

Main conclusions Modelled changes in Deficit between past, present and future climate scenarios suggest that recent past changes in forest structure and composition may accelerate in the future, with species responding individualistically to further declines in water availability. Declining water availability may disproportionately affect *Pinus monticola* and *Tsuga mertensiana*. Fine-scale heterogeneity in soil water-holding capacity, aspect and slope implies that plant water balance may vary considerably within the grid cells of kilometre-scale climate models. Sub-grid-cell soil and topographical data can partially compensate for the lack of spatial heterogeneity in gridded climate data, potentially improving vegetation-change projections in mountainous landscapes with heterogeneous topography.

Keywords
California, climate change, forest vegetation, Little Ice Age, *Pinus monticola*, PRISM, Sierra Nevada, species range shifts, Thornthwaite method, *Tsuga mertensiana*.

Correspondence: James A. Lutz, College of the Environment, University of Washington, Box 352100, Seattle, WA 98195-2100, USA. E-mail: jlutz@u.washington.edu

INTRODUCTION

Many landscape-scale vegetation studies use physical site characteristics as proxies for the environmental variables that directly affect vegetation. Early classifications of forest communities of the Sierra Nevada, California relied on graphical interpretation of data based on elevation (Klyver, 1931). Recent studies have used a generalized gradient based on moisture and temperature (Rundel *et al.*, 1977; Vankat, 1982; Parker, 1989). Although descriptive depictions of these physical gradients capture the general distributions of vegetation on the landscape, calculations more closely related to plant ecophysiology should, in theory, have the potential to better explain finer-scale variation in plant presence (Stephenson, 1998). Ecophysiological field studies have confirmed that water balance determines community leaf area, and that tree water balance is correlated with site conditions (Waring & Cleary, 1967; Hinckley & Scott, 1971; Hinckley & Ritchie, 1972; Grier & Running, 1977). Understanding fine-scale heterogeneity of complex terrain and how this heterogeneity affects plant water balance is increasingly important to understanding the potential effects of climate change on species distributions.

Outputs from climate models are often used to explain distributions of species or vegetation types, but the resulting climate envelopes can have very coarse spatial scales. Forest vegetation differs visibly at spatial scales finer than the grid sizes of most existing climate models – generally about 1 km^2. Furthermore, general circulation models (GCM) used to project the effects of climate change on temperature and precipitation use even larger grid sizes (e.g. $\approx$150 km^2, even when downscaled to a 1/8° grid; Hayhoe *et al.*, 2004). The effect of sub-grid-scale landscape heterogeneity on species distribution will be important to differentiate between species extirpations in a given grid cell, or retreat to small, sub-grid cell refugia.

Although quantitative values for the heating due to solar insolation have been applied based on scaling of slope and aspect (Parker, 1982, 1989), soil data have only recently become digitally available with sufficient spatial resolution and geographic extent to tie slope- and aspect-derived insolation to soil moisture and thus to plant water balance (Dyer, 2009). With the existence of accurate, spatially explicit data for soils and meteorology in mountainous terrain, analyses can now estimate quantitative variation in soil water-holding capacity and air temperature that more directly control plant distribution.

Annual actual evapotranspiration (AET) and annual climatic water deficit (Deficit; *sensu* Stephenson, 1998) can be used to predict vegetation presence (Stephenson, 1990, 1998; McKenzie *et al.*, 2003; Gavin & Hu, 2006) and growth rates (Dyer, 2004; Littell *et al.*, 2008). Following Thornthwaite & Mather (1955) and Stephenson (1990, 1998), we define AET as evaporative water loss from a site covered by a hypothetical standard crop, constrained by the current water availability. AET can be considered a proxy for site net primary productivity (Rosenzweig, 1968) because AET represents the simul-taneous availability of biologically usable energy and water (Stephenson, 1998). Deficit represents the difference between potential evapotranspiration (PET) and AET.

Because soil water-holding capacity, slope and aspect contribute to plant water balance, we sought to incorporate the most recent data and techniques for these inputs into pre-existing methods. Modelling of species presence elsewhere in western North America (McKenzie *et al.*, 2003; Gavin & Hu, 2006) approximated soil water-holding capacity as gridded to the same resolution as climate, or as a uniform value. Previous studies in the Sierra Nevada (Stephenson, 1998; Urban *et al.*, 2000) considered soil water-holding capacity categorically, but these approximations for soil water storage cannot easily be extended to the full range of variation present at a landscape scale. As soil depth and type are often correlated with landscape position, spatially explicit data for air temperature, precipitation and soil water-holding capacity allow calculation of seasonal soil water balance in a manner that follows topography.

Water availability to plants at a site is determined by a nonlinear combination of water supply, soil water storage, water demand and water loss. The amount of precipitation, the proportion falling as snow, and the timing of the snow melt determine the water supply at a site (Stephenson, 1990, 1998). Vegetation (modelled as a hypothetical standard crop), temperature, solar radiation, relative humidity, wind speed and surface roughness determine the water demand. The prolonged summer dry season in the Sierra Nevada decreases the availability of water during the period when light and temperature conditions are most favourable for photosynthesis (Stephenson, 1998; McKenzie *et al.*, 2003). van Mantgem & Stephenson (2007) found that increases in Deficit increase tree mortality in the Sierra Nevada, and van Mantgem *et al.* (2009) found that widespread increases in tree mortality were associated with drier climate on decadal time scales. Earlier snowmelt could increase Deficit on sites with shallow soils; evapotranspiration would start earlier in the season, and evapotranspiration would deplete soil water sooner, thereby decreasing growing periods (Royce & Barbour, 2001a,b). Conversely, more summer precipitation could alleviate drought stress considerably.

Between approximately AD 1650 and 1850, the Sierra Nevada experienced a period of cool and dry temperatures – the local manifestation of the Little Ice Age northern hemispheric cooling (Stine, 1996). This period, from 360 to 160 years ago, corresponds to the inferred establishment dates of many dominant trees in Yosemite, although older trees would have established in the warmer and wetter period before 1650 (Stine, 1996; Van Pelt, 2001). The trees that now represent the forest canopy would therefore have experienced their period of rapid growth during the different climatic conditions of the Little Ice Age. We expected that the warming of the Sierra Nevada since the Little Ice Age has already increased the water stress that has been linked to higher levels of tree mortality (van Mantgem & Stephenson, 2007; van Mantgem *et al.*, 2009). The increase in Deficit between the Little Ice Age and

the present cannot have been extreme with respect to the environmental tolerances of trees, because young and old trees are found together. However, if Deficit increases markedly due to climate change in the future, rates of tree mortality could increase beyond present values.

Our objectives were to calculate climatic water balance within Yosemite National Park, to describe distributions for the most abundant tree species with respect to water-balance variables, and to examine how changes in the water balance may affect species ranges by mid-century. We sought to calculate the water balance using the inherent spatial variability of each input, so that our results would be relevant to complex topography and transferable to other forest ecosystems.

MATERIALS AND METHODS

Study site: physical environment and vegetation

Yosemite National Park covers 3027 km^2 (latitude 37.7° N, longitude 119.7° W) and has been protected since 1890 (Russell, 1992). Elevation ranges from 657 to 3997 m, and although elevation rises gradually from the west to the crest of the Sierra Nevada in the east, local topography is highly variable.

Vegetation in Yosemite National Park is characteristic of the central Sierra Nevada (van Wagtendonk & Fites-Kaufman, 2006) and comprises a mosaic of species and structural stages (Franklin & Fites-Kaufman, 1996). Six major vegetation types have been described: subalpine coniferous forest; upper montane coniferous forest; lower montane coniferous forests;

broadleaved upland forests and woodlands; scrub and chaparral communities; grassland, meadow and herb communities (Fig. 1). A seventh vegetation type comprises those areas with < 20% vegetation. These predominantly unvegetated areas cover ≈ 16% of the park, but isolated trees or tree islands are found.

Fire is an important factor in the distribution and abundance of tree species in Yosemite. Forests burn with a mixture of severities and with median fire-return intervals of 4–187 years, depending on elevation and forest type (van Wagtendonk *et al.*, 2002; Sugihara *et al.*, 2006). A policy of total fire suppression began around 1900 and continued until the early 1970s. Three-quarters of a century of fire exclusion has allowed some forests to develop a 'fire debt' – uncharacteristic species composition, higher density, increased patch connectivity and higher fuel loading (Vale, 1987; Gruell, 2001; van Wagtendonk & Lutz, 2007; Lutz *et al.*, 2009b). These changes constitute an increase in vegetative demand for water superimposed on the underlying climate-driven water supply and standardized evaporative demand.

Plot data

The earliest extensive vegetation data for Yosemite National Park were collected by teams led by Albert E. Wieslander between 1932 and 1936 (Wieslander, 1935; Keeler-Wolf, 2007). The Wieslander survey mapped forest cover throughout California, and included vegetation plots in representative areas of all forest types. Field crews were instructed to select representative plots within the boundary of well-defined
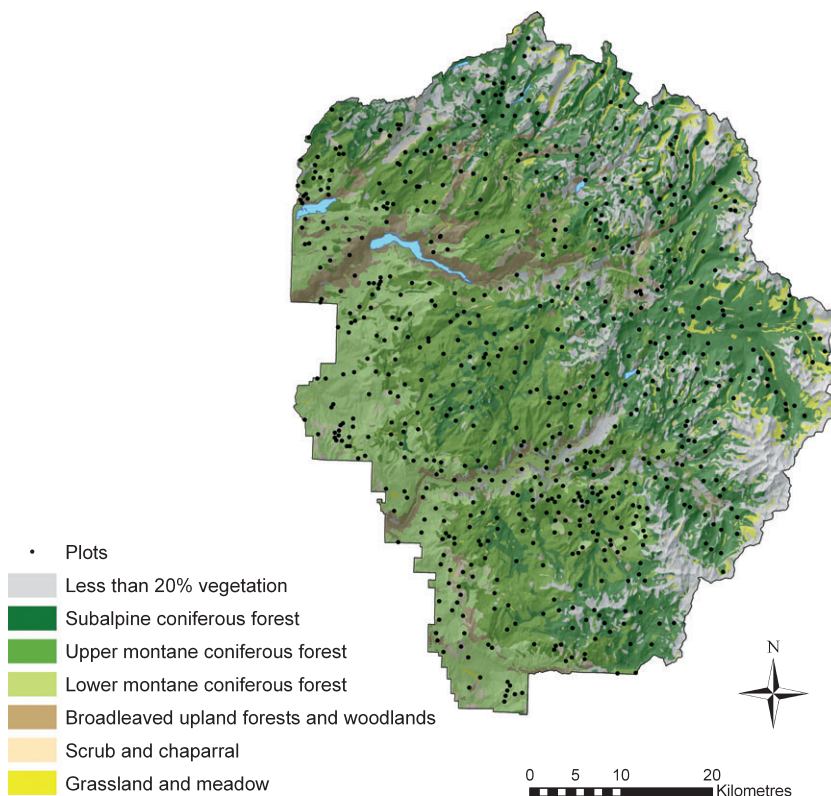

- Plots
- ☐ Less than 20% vegetation
- ■ Subalpine coniferous forest
- ■ Upper montane coniferous forest
- ■ Lower montane coniferous forest
- ■ Broadleaved upland forests and woodlands
- ☐ Scrub and chaparral
- ■ Grassland and meadow

Figure 1 The seven major formations within Yosemite National Park. Continuous vegetation covers ≈ 84% of the 3027 km^2, and includes subalpine coniferous forest, upper montane coniferous forest, lower montane coniferous forest, broadleaved upland forests and woodlands, scrub and chaparral, and grassland and meadow communities. The remaining 16% has less than 20% vegetation cover. The 655 forest plots are distributed throughout the vegetation types of the park.

associations. The survey protocol used 0.2-acre (809.4-m^2) rectangular plots. Live and dead trees were tallied in four diameter classes: 10–30, 31–60, 61–91 and ≥ 92 cm (converted from data sheet values: 4–11″, 12–23″, 24–35″ and ≥ 36″). Areas with < 20% vegetative cover were not sampled; therefore tree species occurring in areas of low vegetative cover (e.g. *Pinus jeffreyi* and *Juniperus occidentalis*) were likely to have been undersampled. Plot locations were transferred from the original survey maps to a geographic information system by the park and georectified by Walker (2000). Physical plot attributes (slope and aspect) were taken from field notes. Species nomenclature follows the *Flora of North America* (Flora of North America Editorial Committee, 1993–2007).

Temperature and precipitation data

Orographic effects over the 3340-m elevation range in Yosemite National Park are large, and single-station meteorological measurements cannot represent the spatial variation present in temperature and precipitation. Therefore we obtained monthly climatological averages from 1971 to 2000 of precipitation and temperature data at 30 arc-second grid size (≈800-m grid cells) from the PRISM climate-mapping project (PRISM, 2007; Daly *et al.*, 2008). PRISM combines data from the National Weather Service Cooperative Observer Program, the Natural Resources Conservation Service snow-courses and Snow Telemetry (SNOTEL), California Data Exchange Stations, and USDA Forest Service Remote Automated Weather Stations. PRISM uses the measured meteorological values to interpolate monthly precipitation, monthly mean maximum temperature and monthly mean minimum temperature for the entire area. There are 55 locations (meteorological stations or snowcourses) with data that contributed to the derived values for at least portions of Yosemite National Park: 36 sources within the park boundaries and an additional 19 meteorological sources within a 10-km buffer zone (Daly *et al.*, 2008; Lutz, 2008; C. Daly, Oregon State University, pers. comm.).

PRISM considers meteorological phenomena relevant to mountainous terrain (e.g. temperature inversions, topographical barriers, the effects of air flow through terrain, and cold air drainages), and may offer improvements over the WorldClim (Hijmans *et al.*, 2005) and Daymet (Running *et al.*, 1987; Thornton *et al.*, 1997) models in some portions of the western USA (Daly *et al.*, 2008). The park contains 4652 grid cells of precipitation and temperature data. The range of precipitation values extracted from PRISM data (804–1722 mm yr^{-1}) is larger than previously reported for the park, and the PRISM values help explain the long-recognized spatial variation in precipitation (Parker, 1995; Urban *et al.*, 2000) better than the low-elevation meteorological stations. Varying largely with elevation, January mean minimum temperatures range from −13.7 to 1.2°C. July mean maximum temperatures range from 13.5 to 34.6°C. The overall annual range in mean monthly temperatures (January minima to July maxima) was 48.3°C across all elevations.

Soil data

Recent soil maps and data were obtained from the Natural Resources Conservation Service (NRCS, 2007). In Yosemite, areas of continuous soil type were mapped to a resolution of 0.4 ha near developed areas and to 16 ha in remote areas. For each soil type, Soil Data Viewer 5.1 (NRCS, 2006) was used to extract information relevant to water-holding capacity. We used the depth to restrictive layer and available water-holding capacity values to determine total available soil water in the soil profile (≤ 200 cm). There were 1687 soil polygons representing 120 soil types. Average available soil water-holding capacity to 200 cm depth among the 655 plots was 91 mm (σ = 54 mm; minimum 32 mm; maximum 342 mm).

Data reduction and analysis

We combined previous methods to calculate AET and Deficit, and used the AET and Deficit values to construct a climate envelope for each species (Thomas *et al.*, 2004; McKenney *et al.*, 2007). We used a Thornthwaite-type water-balance model to calculate climatic water deficit (Thornthwaite, 1948; Thornthwaite & Mather, 1955; Hamon, 1963; Willmott *et al.*, 1985; Dingman, 2002). Although various methods exist for computing water balance, Thornthwaite-type methods are most appropriate when data are limited to temperature and precipitation (Vörösmarty *et al.*, 1998). In a comparative study in the south-eastern USA, Lu *et al.* (2005) found that the Hamon method (a refinement of the Thornthwaite method; Hamon, 1963) was the most accurate when the inputs were limited to these data. Similarly, Vörösmarty *et al.* (1998) found that the Hamon method had the smallest bias over a range of conditions. Dingman (2002) concluded that the Hamon (1963) equations are optimal when only temperature and precipitation data are available. Incorporating wind speed, humidity and net radiation (*sensu* Penman-Monteith; Penman, 1948) may improve the accuracy of the PET calculation, but these data are rarely available in forest ecosystems.

In a Thornthwaite-type water-balance model, water is considered either to be stored in the soil or snowpack, transpired by the vegetation, or evaporated from the soil, or to be surplus that provides runoff. Inputs to the calculations include latitude, mean monthly precipitation, mean monthly temperature and soil water-holding capacity. For temperature and precipitation data, we used the 30-year averages from the PRISM project. Our PET calculation follows Hamon (1963) as refined by Dingman (2002) (see Appendix S1 in Supporting Information). Thornthwaite-type methods were developed for flat terrain. Stephenson (1998) approximated the effects of slope and aspect on PET in complex topography as a multiplicative scalar (+10% for extreme south-facing slopes and −10% for extreme north-facing slopes). Instead of fixed values, we used a dimensionless heat-load index developed by McCune & Keon (2002). They used equations for direct radiation based on latitude, slope and aspect to develop a heat-load index (HL), which reflects the greater temperatures and

evaporative demands in the afternoon by transforming aspect from a north–south axis to a north-east–south-west axis. Our plot data fell within the range of McCune & Keon's (2002) most accurate equation ($0° \leq$ slope $\leq 60°$; $30° \leq$ latitude $\leq 60°$). More recent work (McCune, 2007) has improved the predictive power (from $r^2 = 0.983$ to $r^2 > 0.99$) using nonparametric multiplicative regression, but we used the continuous equations to increase the transferability of the methods. We used the HL values to scale the PET values calculated based on the Thornthwaite assumption of flat terrain. Values for AET and Deficit used here refer to the annual sum of the monthly values calculated (Appendix S1).

For each plot, we calculated AET and Deficit based on the data values from each input layer. Then, for each species present in four or more plots, we calculated mean and range of AET and Deficit based on the characteristics of each plot where the species was present.

North American water-balance ranges of Yosemite tree species

We hypothesized that an increasing summer Deficit might affect some Yosemite tree species, provided that the water balance was a limiting factor driving their presence within the park. To assess the degree to which water balance might be limiting tree presence within Yosemite, and therefore the relative sensitivity of species ranges to increases in Deficit, we compared water-balance parameters of the Yosemite plots with those of the North American range limits of each species (Thompson *et al.*, 1999; Thompson & Anderson, 2000). Thompson *et al.* (1999) examined the entire North American range of abundant tree species within 25-km grid cells (area 625 km^2, approximately one-quarter of Yosemite National Park), and inferred their continental water-balance range from plot data. Thompson *et al.* (1999) used AET/PET as a metric of drought, rather than Deficit. We calculated AET/PET for the plots in Yosemite and compared those results with the species ranges of AET/PET throughout North America, using data from Thompson *et al.* (1999) (R. S. Thompson, US Geological Survey and K. H. Anderson, University of Colorado Boulder, pers. comm.). Thompson *et al.* (1999) used a similar method to ours for calculating AET and PET. However, their study was based on climatological means from 1951 to 1980, and the spatial extent of their grid cells did not permit consideration of heterogeneity in soil water-holding capacity, slope and aspect (at 625 km^2 average aspect approaches flat and slope approaches zero).

Modelling the effects of climate change

We hypothesized that relative similarity in tree composition between the Little Ice Age and the present (as evidenced by the persistence of trees that established in the Little Ice Age) would be partially due to similarities in the water balance between the Little Ice Age and the present. Furthermore, we hypothesized that recent indications of increases in tree mortality (van Mantgem & Stephenson, 2007; Breshears *et al.*, 2009; van Mantgem *et al.*, 2009) could represent the beginning of a shift to the future climate (particularly one with higher Deficit). We compared the magnitude of change in Deficit between the onset of the Little Ice Age and the present with the magnitude of the change in Deficit between present climate and projected future climate. To establish our climate baseline, we used our model to calculate Deficit based on the PRISM climatological means (1971–2000) for each plot (PRISM, 2007). We then developed past and future scenarios from proxies and climate projections (Thompson *et al.*, 2008; Battisti & Naylor, 2009).

Because we wanted to calculate Little Ice Age Deficit for all tree species at all elevations, we did not use climate proxies developed from high-elevation tree chronologies (e.g. *Pinus balfouriana*; Graumlich, 1993) or from tree species with limited distribution (e.g. *Sequoiadendron giganteum*; Swetnam, 1993). Instead, we estimated past temperature by using climate proxies derived from Northern Hemisphere borehole temperature data (Huang *et al.*, 2000; Juckes *et al.*, 2007). Huang *et al.* (2000) determined that annually averaged temperatures in the Northern Hemisphere were 1°C colder in 1700 than in 2000. Accordingly, for every plot, we decreased the temperatures derived from the present PRISM model by 1°C for each month.

To estimate past precipitation, we used data from hydrographically closed Mono Lake, located directly east of Yosemite in the Great Basin (Stine, 1990, 1996). Stine (1990) found that during the Little Ice Age, there were prolonged periods when precipitation east of the Sierra Nevada crest was 79% of the present precipitation, with decadal periods of drier conditions. Accordingly, to model precipitation *c.* 1700 we decreased PRISM-derived values for each plot by 25% (Stine, 1990, 1996; S. Stine, California State University Hayward, pers. comm.; Graham & Hughes, 2007).

In a similar manner, we examined a future climate scenario developed by Hayhoe *et al.* (2004). We took the mean of the results for the Intergovernmental Panel on Climate Change (IPCC) B1 emission scenario (Nakićenović *et al.*, 2000) for the Parallel Climate Model (PCM; Washington *et al.*, 2000) and the Hadley Centre Climate Model version 3 (HadCM3; Gordon *et al.*, 2000; Pope *et al.*, 2000). Based on the average of PCM and HadCM3 models, Hayhoe *et al.* (2004) project an average annual temperature increase of 1.5°C throughout California for the period 2020–49. Accordingly, to calculate Deficit under this climate projection, we increased mean monthly temperatures for each plot by 1.5°C and left mean monthly precipitation unchanged from present values. We compared the present and future scenarios in terms of their absolute changes in Deficit and also relative to the current species ranges. Because species tolerate different ranges of Deficit as well as different mean values, we compared the relative effect of an increase in Deficit by normalizing each species range to mean 0, SD 1, then examining the modelled change in Deficit relative to the standard deviation of each species' current Deficit range.

RESULTS

We used 655 plots containing 16,460 live trees $\geq$ 10 cm d.b.h. representing 22 species, of which 17 species were represented in $\geq$ 4 plots (Fig. 1; Table 1). Plot elevations ranged from 1219 to 3505 m. The heat-load index varied between 0.571 and 1.075 ($\bar{x} = 0.941$, $\sigma = 0.093$). Based on the 1971–2000 climatological means, soils were always below field capacity from July to September. By November, 407 of 655 plots were at field capacity. However, for 192 plots, soil water storage was not at field capacity until the melting of the snowpack in April or May.

The relationship between physical variables (temperature and precipitation) and AET and Deficit generally lay on a gradient defined by two characteristic patterns (Fig. 2). In lower montane coniferous forests, mean monthly temperatures were above 0°C in 11–12 months (Fig. 2, left; Table 2), and the annual trend in AET followed soil water availability: highest from October to June. Beginning in June, available soil water decreased, Deficit increased, and AET was lower. In upper montane coniferous forests, mean monthly temperatures were below 0°C for 2 months or longer (Fig. 2, right; Table 2), AET

Table 1 Trees observed in Yosemite National Park with their frequencies of occurrence (proportion of plots) and total numbers of trees during the Wieslander survey (1932–36); limited to trees with d.b.h. $\geq$ 10 cm.

Species	Family	Proportion of plots (%) $n = 655^*$	Number of trees $n = 16,460†$
Gymnosperms			
Abies concolor	Pinaceae	24.3	1712
Abies magnifica	Pinaceae	29.9	2916
Calocedrus decurrens	Cupressaceae	14.4	478
Juniperus occidentalis	Cupressaceae	7.2	223
Pinus albicaulis	Pinaceae	9.2	680
Pinus contorta	Pinaceae	41.2	4912
Pinus jeffreyi	Pinaceae	25.0	918
Pinus lambertiana	Pinaceae	15.0	437
Pinus monophylla	Pinaceae	0.2	8
Pinus monticola	Pinaceae	19.8	788
Pinus ponderosa	Pinaceae	11.0	658
Pinus sabiniana	Pinaceae	0.8	18
Pseudotsuga menziesii	Pinaceae	2.4	140
Sequoiadendron giganteum	Cupressaceae	0.6	14
Tsuga mertensiana	Pinaceae	15.7	1608
Angiosperms			
Acer macrophyllum	Aceraceae	0.3	13
Alnus incana tenuifolia	Betulaceae	0.3	19
Cornus nuttallii	Cornaceae	0.2	4
Populus tremuloides	Salicaceae	1.4	140
Quercus chrysolepis	Fagaceae	4.4	453
Quercus kelloggii	Fagaceae	8.5	290
Umbellularia californica	Lauraceae	0.3	31

*Total number of plots with live trees $\geq$ 10 cm d.b.h.
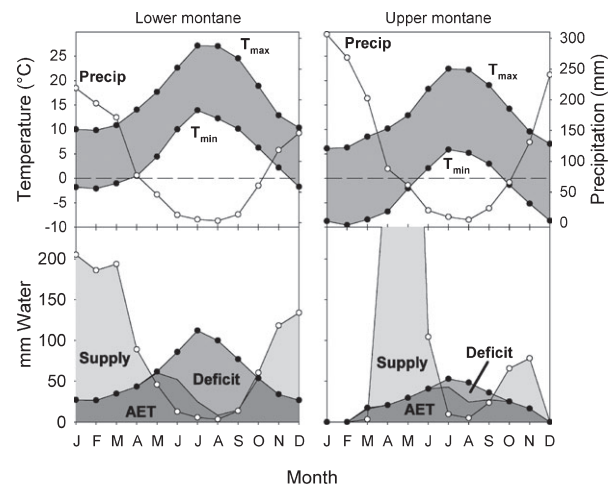†Total number of trees $\geq$ 10 cm d.b.h.

Figure 2 Physical characteristics for a plot in the lower montane coniferous forest (left) and a plot in the upper montane coniferous forest (right) of Yosemite National Park. These two sites have similar soil water capacities, but different elevations, slopes and aspects (Table 2). In the lower montane coniferous forest (left), temperature minima and maxima are mostly above freezing (left, above). Water supply (rain plus snowmelt, lower left, open circles) exceeds evaporative demand (potential evapotranspiration or PET, closed circles) from October to early May. In the upper montane coniferous forest (right), mean monthly temperature is below 0°C from mid November to March (upper right). Water supply peaks at 793 mm in May (lower right). Values calculated from PRISM climatological means (1971–2000).

Table 2 Physical attributes, annual climatic water deficit and annual actual evapotranspiration for the lower montane and upper montane coniferous forest plots in Yosemite National Park shown in Fig. 2.

Parameter	Lower montane coniferous forest	Upper montane coniferous forest
Elevation (m)	1582	2591
Aspect	South-west	North-east
Slope	9°	22°
Heat load factor*	1.025	0.708
Soil water capacity† (mm)	80	80
Annual precipitation‡ (mm)	1066	1422
Jul. max. temperature‡ (°C)	27.14	22.40
Jul. min. temperature‡ (°C)	13.90	5.86
Jan. max. temperature‡ (°C)	10.01	6.08
Jan. min. temperature‡ (°C)	−1.82	−8.78
Annual Deficit (mm)	276	43
Annual AET (mm)	406	243
Species with individuals $\geq$ 10 cm d.b.h. and density (trees ha^{-1})§	CADE (49) PILA (24) PIPO (162)	ABMA (346)

*McCune–Keon heat load factor (see Materials and Methods).
†Soil water-holding capacity in top 200 cm of soil profile.
‡Climatological averages from 1971 to 2000.
§Tree species: CADE (*Calocedrus decurrens*), PILA (*Pinus lambertiana*), PIPO (*Pinus ponderosa*), ABMA (*Abies magnifica*).

was zero during the cold months, and soil water was available and usable from March to November. Soil moisture decreased in the summer, but not as rapidly as in warmer sites.

Species were distributed along axes of AET and Deficit (Fig. 3). *Pinus sabiniana* occupied sites with the highest levels of Deficit, and *Pinus albicaulis* sites with the lowest levels of Deficit. Generally, higher levels of Deficit were associated with lower elevation, but soil water-holding capacity was an important differentiating factor (Table 3). At higher levels of AET and Deficit, AET showed less variation and Deficit became relatively more important in differentiating among species (Fig. 3; Table 3). Individuals of some species (e.g. *Pinus contorta* and *Calocedrus decurrens*) occurred over broad ranges of AET and Deficit, and individuals of some species (e.g. *Sequoiadendron giganteum* and *Pinus sabiniana*) occurred within narrow ranges, partially due to the small number of plots where individuals were present. Species had recognizable annual water-balance patterns. *Pinus ponderosa* (Fig. 4) occupied sites with a mediterranean climate, with readily available soil water throughout the winter months and a period of prolonged summer drought. *Pinus albicaulis* (Fig. 4) occupied sites characterized by long winters during which AET was zero followed by a rapid snowmelt and cool summers. *Abies concolor* and *Abies magnifica* were intermediate species, and the AET–Deficit relationship (Fig. 4) shows that *Abies magnifica*
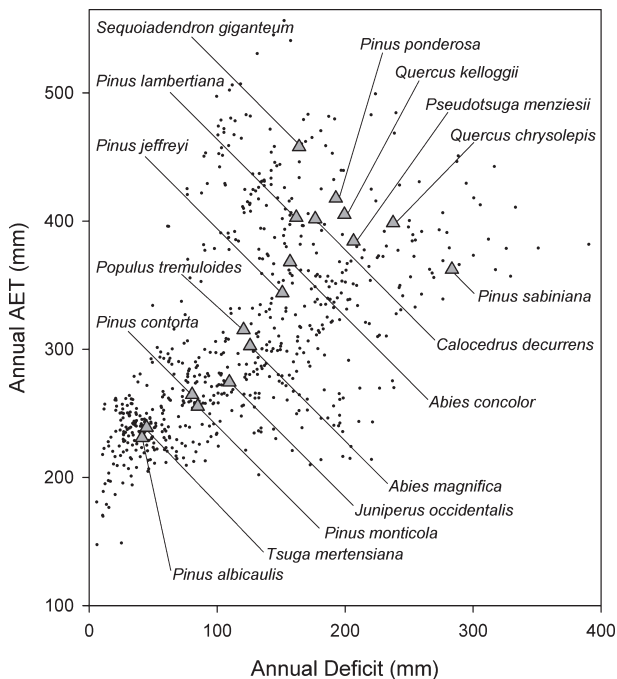
Table 3 Characteristic means of elevation, soil water-holding capacity, annual AET and annual Deficit for the 17 tree species found in ≥ 4 plots in Yosemite National Park.

Species	Elevation (m)	Soil water capacity (mm)	Annual AET (mm)	Annual Deficit (SD) (mm)
Abies concolor	2083	113	368	157 (47)
Abies magnifica	2426	83	303	126 (50)
Calocedrus decurrens	1763	130	402	177 (66)
Juniperus occidentalis	2449	72	274	110 (59)
Pinus albicaulis	3018	79	231	41 (24)
Pinus contorta	2694	77	265	80 (52)
Pinus jeffreyi	2199	98	344	151 (48)
Pinus lambertiana	1911	136	403	162 (52)
Pinus monticola	2680	70	255	85 (47)
Pinus ponderosa	1680	139	418	193 (69)
Pinus sabiniana	1463	43	362	283*
Populus tremuloides	2360	90	315	121*
Pseudotsuga menziesii	1564	92	384	207 (53)
Quercus chrysolepis	1556	98	399	237 (77)
Quercus kelloggii	1704	123	405	199 (69)
Sequoiadendron giganteum	1966	166	458	164*
Tsuga mertensiana	2824	73	239	45 (25)

*Standard deviation was not calculated for species found in less than 10 plots.

occupied sites that were colder and snowier than those occupied by *Abies concolor*. The AET–Deficit relationship differentiated among species that occur at similar elevations. *Sequoiadendron giganteum*, *Pinus lambertiana* and *Abies concolor* co-occur in the lower montane mixed conifer forest types. Differences among them were partly explained by the differences in the mean soil water-holding capacity (Table 3). *Sequoiadendron giganteum* (mean elevation 1966 m) occupied sites with greater soil water-holding capacity (166 mm) than *Pinus lambertiana* (mean elevation 1911 m, mean soil water-holding capacity 136 mm) or *Abies concolor* (mean elevation 2083 m, mean soil water-holding capacity 113 mm).

Species comparison of Yosemite water balance to North American range

With respect to the water-balance metric AET/PET, most species in Yosemite were found on sites in either the middle or drier portion of the North American range for that species (Fig. 5).

Values for AET/PET in Yosemite for *Pinus sabiniana*, *Quercus chrysolepis*, *Pinus jeffreyi*, *Populus tremuloides*, *Juniperus occidentalis*, *Pinus contorta* and *Pinus albicaulis* were well within the North American water-balance envelope for each species, with values of AET/PET throughout North America extending both above and below the values in Yosemite. Sites in Yosemite occupied by *Pseudotsuga menziesii*, *Quercus*
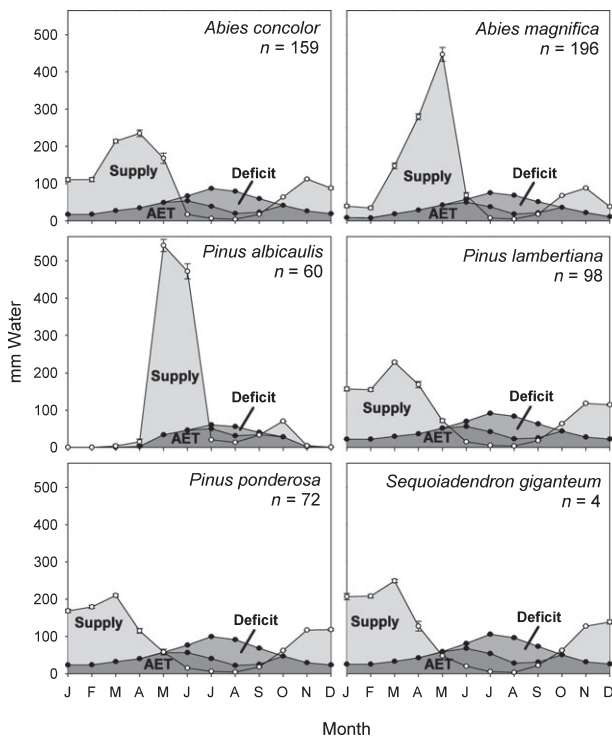

Figure 3 Tree distribution in Yosemite National Park. Annual Deficit and annual actual evapotranspiration (AET) are shown for each plot where trees ≥ 10 cm d.b.h. were present (*n* = 655; small dots). Species means of Deficit and AET for species with frequency ≥ 4 plots are shown with triangles. Species means represent all plots where each species was found without regard to the within-plot abundance. Values calculated from PRISM climatological means (1971–2000).

Figure 4 Characteristic water-balance relationships for six tree species in Yosemite National Park. Winter temperatures, spring water supply and soil water-holding capacity combine to determine Deficit and actual evapotranspiration (AET) (mean ± SE). Water-balance curves are based on means of plots where these species were present. Among species at similar elevations, increased soil water-holding capacity results in higher AET (Fig. 2; Table 2). Values calculated from PRISM climatological means (1971–2000).

kelloggii, *Pinus ponderosa*, *Calocedrus decurrens*, *Pinus lambertiana*, *Abies concolor* and *Abies magnifica* were clustered towards the arid end of the North American range for those species; but within the North American range, each species was found on some sites with lower AET/PET than those in Yosemite (Fig. 5). Sites in Yosemite occupied by *Pinus monticola* and *Tsuga mertensiana* were among the most arid recorded for those species in North America (Fig. 5). Continental water-balance metrics were not available for *Sequoiadendron giganteum*.

Climate change projections

Modelled results from the three different time periods (Little Ice Age, present and mid-21st century) allowed us to compare the relative magnitude of change from past climate to present climate, and from present climate to the future climate scenario. The change from the cool and dry Little Ice Age climate to the warmer and wetter present climate changed both water supply and water demand. Warmer present temperatures compared with Little Ice Age temperatures increased modelled evaporative demand, but increased precipitation decreased the

period over which soils were depleted of available water. The combined effect was a modelled increase in Deficit of 5% across all plots (Table 4). Deficit increased ≥ 5% between the Little Ice Age and the present for plots occupied by *Abies concolor*, *Abies magnifica*, *Juniperus occidentalis*, *Pinus jeffreyi*, *Pinus monticola* and *Populus tremuloides*. Deficit decreased ≥ 5% for plots occupied by *Pinus albicaulis*, *Sequoiadendron giganteum* and *Tsuga mertensiana*. There was an average modelled increase in AET of 12% across all plots.

In contrast, the change in modelled Deficit from present climate to future climate scenario was much greater than the change in Deficit from Little Ice Age to present (Table 4). The increases in temperature projected by Hayhoe *et al.* (2004) decreased snowpack and increased summer PET, resulting in modelled increases in Deficit of 23% across all plots (Table 4). Modelled Deficit increased ≥ 25% for plots occupied by *Abies magnifica*, *Juniperus occidentalis*, *Pinus albicaulis*, *Pinus contorta*, *Pinus monticola*, *Sequoiadendron giganteum* and *Tsuga mertensiana*. When the increase in Deficit for each species was expressed in terms of the standard deviation of that species' Deficit in the present climate, the increase in Deficit between the present and future scenario ranged from 0.46σ to 0.76σ (mean 0.56σ) for species present in ≥ 10 plots (Fig. 6). Average modelled AET increased 10%. AET/PET changed little for most Yosemite plots.

DISCUSSION

Water-balance methods of predicting tree species presence and abundance have been used in palaeoecological studies (Huntley, 2001; Dyer, 2004), global studies of inter-annual variation in AET (Frank & Inouye, 1994), and climate change projections (Thomas *et al.*, 2004; Kutzbach *et al.*, 2005; McKenney *et al.*, 2007; Grundstein, 2009). With the increasing availability of kilometre-scale climate data and 10- to 100-m-scale data for soils, aspect and slope, calculating landscape scale distributions of water balance becomes increasingly possible, and changes in Deficit become another way to examine the potential effects of climate change scenarios (Figs 3, 5 & 6). Each species has a drought threshold beyond which no growth occurs (Waring & Cleary, 1967; Hinckley & Scott, 1971; Thompson *et al.*, 1999; Royce & Barbour, 2001a). These limits can help us understand the magnitude of vegetation change that may result from climate changes, and to infer the sensitivity of species in a particular location (Hannah *et al.*, 2002). Because some inputs to water-balance calculations are available at resolutions much finer than climatological data or GCM outputs, calculations of AET and Deficit may offer a method to circumvent the downscaling problem in climate change forecasts.

Spatial resolution

Our method allows a straightforward calculation of landscape-wide water balance in different climate scenarios at finer spatial resolution than gridded climate models. Present climate models (Daymet, PRISM) feature kilometre-scale spatial
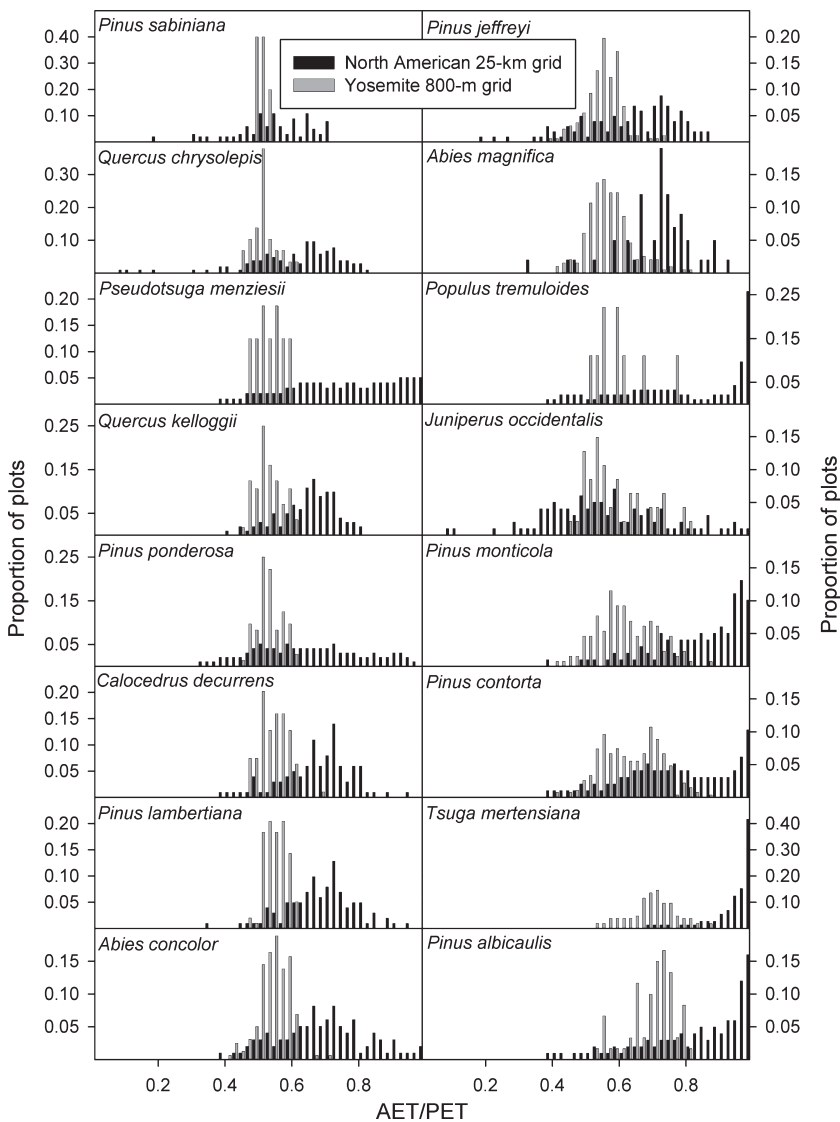
Figure 5 Comparison of water-balance parameters for plots where tree species were found in Yosemite National Park (grey) and throughout North America (black). The water-balance metric for comparison is AET/PET. North American range data are based on plots within 25-km grid cells (area 625 km²). Species are arranged in order of increasing Deficit in Yosemite (note differing vertical scales). North American water-balance data were not available for *Sequoiadendron giganteum*. North American range data courtesy of Katherine Anderson and Robert Thompson (from Thompson *et al.*, 1999).

resolution (1000 m for Daymet, 800 m for PRISM). Global-scale water- and energy-balance models such as the Variable Infiltration Capacity model (Liang *et al.*, 1994; Nijssen *et al.*, 2001) consider input parameters to have the same spatial variation (a uniform grid cell size of 1/8° or 1/16°), and the large spatial scale implies flat terrain with no variation in aspect. These models are typically used for watershed, continental or global analyses of water dynamics (e.g. Sun *et al.*, 2005). They are not designed explicitly to consider the changes in vegetation that can occur within hundreds of metres because they are parameterized by vegetation type (forest, woodland, savanna, etc.) rather than species. However, the spatial variation in slope, aspect, topographic shading and soil water-holding capacity are more precisely known and can vary at finer spatial scales than climate models can resolve (Urban *et al.*, 2000; Kane *et al.*, 2008). The present method retains the spatial resolution of non-gridded inputs (soil water-holding capacity, slope and aspect) and combines them with gridded output from climate models, so that the water-balance calculations reflect the inherent spatial variation of each input.

Data limitations

The climate envelope approach has been used to characterize species presence from known climate, and also to infer past climate from species presence (Huntley, 2001). The climate envelope approach requires an assumption that current species ranges are constrained primarily by climate, and that past and future climates will feature similar climate envelopes for each species. However, as climate changes, interactions among plant species, fire, insects and the climate envelopes may give rise to non-analogue vegetation communities (Brubaker, 1988; Williams & Jackson, 2007; Williams *et al.*, 2007).

Although we consider the Wieslander plot data to be representative of Yosemite vegetation, inferences are limited to the geographical boundaries of the park. Several species have a very limited distribution within the park, and Yosemite represents only a small portion of those species ranges (Fig. 5). For example, *Pinus sabiniana* occupied a relatively narrow elevation band between chaparral and the denser coniferous forests at the park's lowest elevations. Although

Table 4 Mean values for climatic water deficit for modelled climate in the Little Ice Age (c. 1700), present (1971–2000) and future (2020–49) for tree species in Yosemite National Park. Climate data from PRISM (2007).

| Species	Past (c. 1700) (mm)	Present (1971–2000) (mm)	Future (2020–49) (mm)
Abies concolor	149	157	185
Abies magnifica	114	126	157
Calocedrus decurrens	174	177	207
Juniperus occidentalis	96	110	139
Pinus albicaulis	44	41	54
Pinus contorta	77	80	107
Pinus jeffreyi	140	151	179
Pinus lambertiana	157	162	191
Pinus monticola	78	85	117
Pinus ponderosa	190	193	225
Pinus sabiniana	285	283	323
Populus tremuloides	103	121	140
Pseudotsuga menziesii	207	207	240
Quercus chrysolepis	237	237	274
Quercus kelloggii	196	199	232
Sequoiadendron giganteum	174	164	209
Tsuga mertensiana	48	45	64
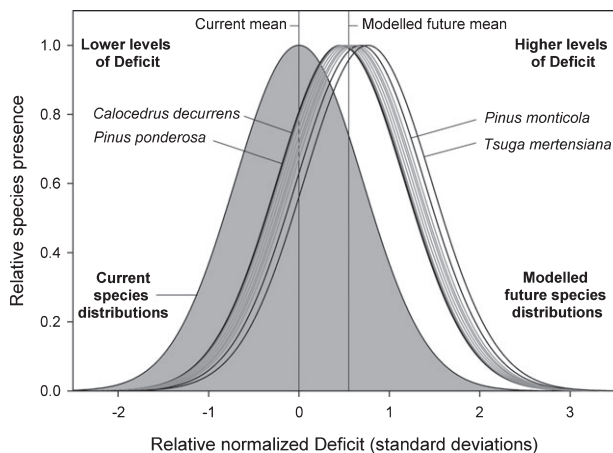
Figure 6 Modelled changes in Deficit from present (1971–2000 means) to future (2020–49) at sites where trees are now found in Yosemite National Park. Current species ranges are approximated by a normal distribution of Deficit, with means (Table 2) normalized to zero and standard deviations (Table 2) normalized to one. Modelled changes in Deficit (Table 3) have been normalized to standard deviation for each species (Table 2). The magnitude of modelled change in Deficit affects species individualistically. *Calocedrus decurrens* and *Pinus ponderosa* were modelled as having the lowest proportional change in Deficit, while *Pinus monticola* and *Tsuga mertensiana* were modelled as having the highest proportional change in Deficit.

Pinus sabiniana tolerates a wide range of water availability, factors other than water balance may ultimately determine which sites this species occupies.

We used current climate data alongside plot data from the 1930s. Low-elevation temperatures in Yosemite (Hetch Hetchy and Yosemite Park Headquarters meteorological stations) increased approximately 0.4°C between the 1930s and the 1990s. This increase in temperatures has been linked to increased mortality of older trees (Lutz *et al.*, 2009a; van Mantgem *et al.*, 2009). However, a comparison of the 655 plots from the Wieslander survey with 210 plots from a modern survey (1988–99) did not find changes in species ranges throughout the park (Lutz, 2008; Lutz *et al.*, 2009a; but see Thorne *et al.*, 2008 for range shifts at lower elevations between the 1930s and 1990s).

Temperature and precipitation averages calculated by the PRISM group consider many factors relevant to mountainous terrain, but some areas have a low density of observed weather to guide the PRISM calculations. Finer-scale temperature variation, especially in valley bottoms (Lundquist *et al.*, 2008), also differentiates vegetation. The NRCS soil map extends to a soil depth of 200 cm, generally sufficient to record the uptake of the approximately 90% of fine roots in the top 50 cm of the soil profile – the most relevant depth for germination and early growth of trees, but this soil map does not yet fully characterize the soil profile. Individual tree variation in response to variations in water balance (Hinckley *et al.*, 1978) and the ability of certain trees to access water through cracks in bedrock (Hubbert *et al.*, 2001) or from overall deeper rooting depth within soil (Waring & Cleary, 1967) suggest that modelling will never be able to explain all the variation in landscape parameters. Thornthwaite-type water-balance models also assume that evapotranspiration is a function of air temperature. However, at higher elevations, cold soils can inhibit water uptake, producing moisture stress when Thornthwaite-type models indicate none (Hinckley & Ritchie, 1972). Field measurements along the environmental gradient of Yosemite during the growing season, and also during the period of maximum water stress, may help characterize species' responses to water stress (Grier & Running, 1977; Royce & Barbour, 2001a).

Fire

Factors other than the site water balance – competitive interactions among species, trophic effects and fire – also limit species ranges. The effect of climate on fire frequency and severity (Swetnam, 1993; McKenzie *et al.*, 2004; Lutz *et al.*, 2009b) may change a species' realized niche more than climate. Our data set includes trees as small as 10 cm d.b.h., and sufficiently frequent fire could eliminate individuals of this size. Sites with high soil moisture deficit will also have dry fuels and may be prone to burn at higher severity if ignited (Lutz *et al.*, 2009b). Other sites are isolated by rock outcroppings, and may provide refuge from most fire events. Fire probably does not play a role in constraining the effect of climate on higher-elevation species (van Wagtendonk & Lutz, 2007) where both Deficit and AET are low. Because AET is an index of site potential for productivity, sites with high AET may be more prone to rapid fuel accumulation. Higher-productivity sites with infrequent

fire will tend to burn at the highest severity. When fire is frequent or severe, species' presence may be limited by dispersal or fire (Urban *et al.*, 2000). AET–Deficit relationships, combined with knowledge of species sensitivities to fire, can help explain how forest communities change when fire is excluded. *Abies concolor* occupies sites with a broad range of AET and Deficit, but can occupy sites with less soil water-holding capacity than pioneer species such as *Sequoiadendron giganteum* (113 vs. 166 mm mean soil water-holding capacity). Because *Abies concolor* is also shade-tolerant, the water-balance relationship emphasizes the importance of fire in keeping *Abies concolor* a minor component of sequoia groves.

Climate change

Changes in Deficit between *c.* 1700 and the present were small (mean increase of 5%) because the increase in temperature was counterbalanced by an increase in precipitation (Table 4). The moderate increase in Deficit does not appear to have altered species ranges yet. But between the mid-1930s and the mid-1990s, most tree species in Yosemite National Park showed declines in their largest diameter classes (Lutz *et al.*, 2009a), with at least a portion of these declines linked to drier conditions (van Mantgem & Stephenson, 2007; van Mantgem *et al.*, 2009). Our modelled results for species that exhibited decreases in Deficit (e.g. *Pinus albicaulis*) are also consistent with these species' higher growth and persistence in the 20th century (Millar *et al.*, 2004).

Our assumptions of equivalent past and present decadal variance in precipitation and temperature are generally confirmed by higher-resolution dendrochronological studies (Graumlich, 1993). However, multi-annual periods of higher or lower temperatures could have caused periods of higher or lower establishment that are reflected in present tree distributions. Climate change projections are subject to considerable modelling uncertainty, and the response of trees may depend more on the patterns of temperature and precipitation extremes rather than on the seasonal means. Furthermore, no general circulation model can discount the possibility of large temperature increases (Roe & Baker, 2007). Our future scenario of increasing temperature with constant precipitation is a conservative assumption; the IPCC B1 emission scenario represents a very small warming compared with more likely emissions pathways (Nakićenović *et al.*, 2000). Our assumption of a 1.5°C mean annual increase understates the increase in Deficit by 1.3% compared with a projection where summer temperatures in the Sierra Nevada increase by an amount higher than the annual average – as the HadCM3 projects (Hayhoe *et al.*, 2004). In addition, both the PCM and the HadCM3 project small decreases in precipitation for California. Therefore our methods are most likely to understate the effect of future climate change on Deficit.

Given the future scenario of 1.5°C higher annual temperatures in the IPCC B1 scenario, there would be a substantial increase in Deficit both in absolute terms (Table 4) and relative to species' current distribution (Fig. 5). A temperature increase – even without a decrease in precipitation – will increase mean evaporative demand, decrease snowpack and thereby increase Deficit. Our modelling showed a significant increase in Deficit for all tree species (Table 4; Fig. 6). The modelled increase in Deficit may be partially offset by the modelled increase in AET in spring and autumn. However, species close to their water-balance range limit (*Pinus monticola* and *Tsuga mertensiana*) may be more affected by the increase in Deficit (Breshears *et al.*, 2009). For other tree species, individual trees that established *c.* 1700 – now generally large – may be at risk of Deficit-related mortality if they are located on sites near the recorded North American range limit for the species. At least some plots currently occupied by *Pseudotsuga menziesii*, *Quercus kelloggii*, *Pinus ponderosa*, *Calocedrus decurrens*, *Pinus lambertiana*, *Abies concolor* and *Abies magnifica* may fall into this category (Fig. 5). Other species (e.g. *Pinus contorta*) occupied sites with broad ranges of environmental parameters and may be less limited by climate than by competition, initial patterns of establishment (Larson & Franklin, 2005), productivity (Larson *et al.*, 2008), intermediate disturbance (Lutz & Halpern, 2006), or other factors (Figs 5 & 6).

While changing climate will allow trees to grow in new locations, development of mature forest cover at plots where the climate becomes permissive depends on seed dispersal, establishment, and a long period of growth. Because climate-induced tree mortality can be rapid and the time for climate-induced tree establishment can be slow, a decrease in older trees in one portion of a species' range occurring over several decades may not be immediately offset by growth elsewhere. Although tree species will vary in sensitivity to changes in Deficit, the modelled change in Deficit in the near future is of much larger magnitude than the changes in the recent past, and even these smaller changes in the recent past have been associated with increased rates of tree mortality. Therefore climate-induced increases in tree mortality may accelerate, affecting species ranges and size distributions.

REFERENCES

Battisti, D.S. & Naylor, R.L. (2009) Historical warnings of future food insecurity with unprecedented seasonal heat. *Science*, **323**, 240–244.

Breshears, D.D., Myers, O.B., Meyer, C.W., Barnes, F.J., Zou, C.B., Allen, C.D., McDowell, N.G. & Pockman, W.T. (2009) Tree die-off in response to global change-type drought: mortality insights from a decade of plant water-potential measurements. *Frontiers in Ecology and the Environment*, **7**, 185–189.

Brubaker, L.B. (1988) Vegetation history and anticipating future climate change. *Ecosystem management for parks and wilderness* (ed. by J.K. Agee and D.R. Johnson), pp. 41–62. University of Washington Press, Seattle, WA.

Daly, C., Halbleib, M., Smith, J.I., Gibson, W.P., Doggett, M.K., Taylor, W.P., Curtis, J. & Pasteris, P.P. (2008) Physiographically-sensitive mapping of climatological temperature and precipitation across the conterminous United States. *International Journal of Climatology*, **28**, 2031–2064.

Dingman, S.L. (2002) *Physical hydrology*. Prentice Hall, Upper Saddle River, NJ.

Dyer, J.M. (2004) A water budget approach to predicting tree species growth and abundance, utilizing paleoclimatology sources. *Climate Research*, **28**, 1–10.

Dyer, J.M. (2009) Assessing topographic patterns in moisture use and stress using a water balance approach. *Landscape Ecology*, **24**, 391–403.

Flora of North America Editorial Committee (1993–2007) *Flora of North America north of Mexico*. Flora of North America Association, New York, NY.

Frank, D.A. & Inouye, R.S. (1994) Temporal variation in actual evapotranspiration of terrestrial ecosystems: patterns and ecological implications. *Journal of Biogeography*, **21**, 401–411.

Franklin, J.F. & Fites-Kaufman, J. (1996) Assessment of late-successional forests of the Sierra Nevada. *Sierra Nevada Ecosystem Project: final report to Congress, Assessments and scientific basis for management options*, pp. 627–661. Centers for Water and Wildland Resources, University of California, Davis, CA.

Gavin, D.G. & Hu, F.S. (2006) Spatial variation of climatic and non-climatic controls on species distribution: the range limit of *Tsuga heterophylla*. *Journal of Biogeography*, **33**, 1384–1396.

Gordon, C., Cooper, C., Senior, C.A., Banks, H., Gregory, J.M., Johns, T.C., Mitchell, J.F.B. & Wood, R.A. (2000) The simulation of SST, sea ice extents and ocean heat transports in a version of the Hadley Centre coupled model without flux adjustments. *Climate Dynamics*, **16**, 147–168.

Graham, N.E. & Hughes, M.K. (2007) Reconstructing the mediaeval low stands of Mono Lake, Sierra Nevada, California, USA. *The Holocene*, **17**, 1197–1210.

Graumlich, L.J. (1993) A 1000-year record of temperature and precipitation in the Sierra Nevada. *Quaternary Research*, **39**, 249–255.

Grier, C.C. & Running, S.W. (1977) Leaf area of mature northwestern coniferous forests: relation to site water balance. *Ecology*, **58**, 893–899.

Gruell, G.E. (2001) *Fire in Sierra Nevada forests: a photographic interpretation of ecological change since 1849*. Mountain Press Publishing Company, Missoula, MT.

Grundstein, A. (2009) Evaluation of climate change over the continental United States using a moisture index. *Climatic Change*, **93**, 103–115.

Hamon, W.R. (1963) *Computation of direct runoff amounts from storm rainfall*. Publication No. 63, pp. 52–62. International Association of Scientific Hydrology, Paris.

Hannah, L., Midgley, G.F., Lovejoy, T., Bond, W.J., Bush, M., Lovett, J.C., Scott, D. & Woodward, F.I. (2002) Conservation of biodiversity in a changing climate. *Conservation Biology*, **16**, 264–268.

Hayhoe, K., Cayan, D., Field, C.B., Frumhoff, P.C., Maurer, E.P., Miller, N.L., Moser, S.C., Schneider, S.H., Cahill, K.N., Cleland, E.E., Dale, L., Drapek, R., Hanemann, R.M., Kalkstein, L.S., Lenihan, J., Lunch, C.K., Neilson, R.P., Sheridan, S.C. & Verville, J.H. (2004) Emissions pathways, climate change, and impacts on California. *Proceedings of the National Academy of Sciences USA*, **101**, 12422–12427.

Hijmans, R.J., Cameron, S.E., Parra, J.L., Jones, P.G. & Jarvis, A. (2005) Very high resolution interpolated climate surfaces for global land areas. *International Journal of Climatology*, **25**, 1965–1978.

Hinckley, T.M. & Ritchie, G.A. (1972) Reaction of mature *Abies* seedlings to environmental stresses. *Transactions of the Missouri Academy of Sciences*, **6**, 24–37.

Hinckley, T.M. & Scott, D.R.M. (1971) Estimates of water loss and its relation to environmental parameters in Douglas-fir saplings. *Ecology*, **52**, 520–524.

Hinckley, T.M., Lassoie, J.P. & Running, S.W. (1978) Temporal and spatial variations in water status of forest trees. *Forest Science*, **24**, 1–72.

Huang, S.P., Pollack, H.N. & Shen, P.Y. (2000) Temperature trends ever the past five centuries reconstructed from borehole temperatures. *Nature*, **403**, 756–758.

Hubbert, K.R., Beyers, J.L. & Graham, R.C. (2001) Roles of weathered bedrock and soil in seasonal water relations of *Pinus jeffreyi* and *Arctostaphylos patula*. *Canadian Journal of Forest Research*, **31**, 1947–1957.

Huntley, B. (2001) Reconstructing past environments for the Quaternary palaeovegetation record. *Biology and Environment: Proceedings of the Royal Irish Academy*, **101B**, 3–18.

Juckes, M.N., Allen, M.R., Briffa, K.R., Esper, J., Hegerl, G.C., Moberg, A., Osborn, T.J. & Weber, S.L. (2007) Millennial temperature reconstruction intercomparison and evaluation. *Climate of the Past*, **3**, 591–609.

Kane, V.R., Gillespie, A.R., McGaughey, R., Lutz, J.A., Ceder, K. & Franklin, J.F. (2008) Interpretation and topographic correction of conifer forest canopy self-shadowing using spectral mixture analysis. *Remote sensing of Environment*, **112**, 3820–3832.

Keeler-Wolf, T. (2007) The history of vegetation classification and mapping in California. *Terrestrial vegetation of California* (ed. by M. Barbour, T. Keeler-Wolf and A.A. Schoenherr), pp. 1–42. University of California Press, Berkeley, CA.

Klyver, F.D. (1931) Major plant communities in a transect of the Sierra Nevada mountains of California. *Ecology*, **12**, 1–17.

Kutzbach, J.E., Williams, J.W. & Vavrus, S.J. (2005) Simulated 21st century changes in regional water balance of the Great Lakes region and links to changes in global temperature and poleward moisture transport. *Geophysical Research Letters*, **32**, L17707, doi:10.1029/2005GL023506.

Larson, A.J. & Franklin, J.F. (2005) Patterns of conifer tree regeneration following an autumn wildfire event in the western Oregon Cascade Range, USA. *Forest Ecology and Management*, **218**, 25–36.

Larson, A.J., Lutz, J.A., Gersonde, R.F., Franklin, J.F. & Heitpas, F.F. (2008) Potential site productivity influences the rate of forest structural development. *Ecological Applications*, **18**, 899–910.

Liang, X., Lettenmaier, D.P., Wood, E.F. & Burges, S.J. (1994) A simple hydrologically based model of land-surface water and energy fluxes for general circulation models. *Journal of Geophysical Research*, **99**, 14415–14428.

Littell, J.S., Peterson, D.L. & Mjoelker, M. (2008) Douglas-fir growth in mountain ecosystems: water limits tree growth from stand to region. *Ecological Monographs*, **78**, 349–368.

Lu, J., Sun, G., McNulty, S.G. & Amatya, D.M. (2005) A comparison of six potential evapotranspiration methods for regional use in the southeastern United States. *Journal of the American Water Resources Association*, **41**, 621–633.

Lundquist, J.D., Pepin, N. & Rochford, C. (2008) Automated algorithm for mapping regions of cold-air pooling in complex terrain. *Journal of Geophysical Research*, **113**, D22107, doi:10.1029/2008JD009879.

Lutz, J.A. (2008) *Climate, fire, and vegetation change in Yosemite National Park*. PhD Thesis, University of Washington, Seattle, WA.

Lutz, J.A. & Halpern, C.B. (2006) Tree mortality during early forest development: a long-term study of rates, causes, and consequences. *Ecological Monographs*, **76**, 257–275.

Lutz, J.A., van Wagtendonk, J.W. & Franklin, J.F. (2009a) Twentieth-century decline in large-diameter trees in Yosemite National Park. *Forest Ecology and Management*, **257**, 2296–2307.

Lutz, J.A., van Wagtendonk, J.W., Thode, A.E., Miller, J.D. & Franklin, J.F. (2009b) Climate, lightning ignitions, and fire severity in Yosemite National Park, California, USA. *International Journal of Wildland Fire*, **18**, 765–774.

van Mantgem, P.J. & Stephenson, N.L. (2007) Apparent climatically induced increase of tree mortality rates in a temperate forest. *Ecology Letters*, **10**, 909–916.

van Mantgem, P.J., Stephenson, N.L., Byrne, J.C., Daniels, L.D., Franklin, J.F., Fulé, P.Z., Harmon, M.E., Larson, A.J., Smith, J.M., Taylor, A.H. & Veblen, T.T. (2009) Widespread increase of tree mortality rates in the western United States. *Science*, **323**, 521–524.

McCune, B. (2007) Improved estimates of incident radiation and heat load using non-parametric regression against topographic variables. *Journal of Vegetation Science*, **18**, 751–754.

McCune, B. & Keon, D. (2002) Equations for potential annual direct incident radiation and heat load. *Journal of Vegetation Science*, **13**, 603–606.

McKenney, D.W., Pedlar, J.H., Lawrence, K., Campbell, K. & Hutchinson, M.F. (2007) Beyond traditional hardiness zones: using climate envelopes to map plant range limits. *BioScience*, **57**, 929–937.

McKenzie, D., Peterson, D.W., Peterson, D.L. & Thornton, P.E. (2003) Climatic and biophysical controls on conifer species distributions in mountain forests of Washington State, USA. *Journal of Biogeography*, **30**, 1093–1108.

McKenzie, D., Gedalof, Z., Peterson, D.L. & Mote, P. (2004) Climatic change, wildfire, and conservation. *Conservation Biology*, **18**, 890–902.

Millar, C.I., Westfall, R.D., Delany, D.L., King, J.C. & Graumlich, L.J. (2004) Response of subalpine conifers in the Sierra Nevada, California, USA, to 20th-century warming and decadal climate variability. *Arctic, Antarctic and Alpine Research*, **36**, 181–200.

Nakićenović, N., Davidson, O., Davis, G., Grüblerr, A., Kram, T., La Rovere, E.L., Metz, B., Morita, T., Pepper, W., Pitcher, H., Sankovski, A., Shukla, P., Swart, R., Watson, R. & Dadi, Z. (2000) *Intergovernmental Panel on Climate Change special report on emissions scenarios*. Cambridge University Press, Cambridge.

Nijssen, B., O'Donnell, G.M., Lettenmaier, D.P., Lohmann, D. & Wood, E.F. (2001) Predicting the discharge of global rivers. *Journal of Climate*, **14**, 3307–3323.

NRCS (2006) *Soil data viewer 5.1 user guide*. USDA Natural Resources Conservation Service, Fort Worth, TX.

NRCS (2007) *Soil survey geographic (SSURGO) database for Yosemite National Park, California, USA* (Soil survey area symbol CA790). http://soildatamart.nrcs.usda.gov (accessed 9 January 2007). USDA Natural Resources Conservation Service, Fort Worth, TX.

Parker, A.J. (1982) The topographic relative moisture index: an approach to soil moisture assessment in mountain terrain. *Physical Geography*, **3**, 160–168.

Parker, A.J. (1989) Forest environment relationships in Yosemite National Park, California, United States. *Vegetatio*, **82**, 41–54.

Parker, A.J. (1995) Comparative gradient structure and forest cover types in Lassen Volcanic National Park and Yosemite National Park, California. *Bulletin of the Torrey Botanical Club*, **122**, 58–68.

Penman, H.L. (1948) Natural evaporation from open water, bare soil and grass. *Proceedings of the Royal Society of London, Series A, Mathematical and Physical Sciences*, **193**, 120–145.

Pope, V.D., Gallani, M.L., Rowntree, P.R. & Stratton, R.A. (2000) The impact of new physical parameterizations in the

Hadley Centre climate model: HadAM3. *Climate Dynamics*, **16**, 123–146.

PRISM (2007) *Climatological normals, 1971–2000*. The PRISM Group, Oregon State University, Corvallis, OR.

Roe, G.H. & Baker, M.B. (2007) Why is climate sensitivity so unpredictable? *Science*, **318**, 629–632.

Rosenzweig, M.L. (1968) Net primary productivity of terrestrial communities: prediction from climatological data. *The American Naturalist*, **102**, 67–74.

Royce, E.B. & Barbour, M.G. (2001a) Mediterranean climate effects. I. Conifer water use across a Sierra Nevada ecotone. *American Journal of Botany*, **88**, 911–918.

Royce, E.B. & Barbour, M.G. (2001b) Mediterranean climate effects. II. Conifer growth phenology across a Sierra Nevada ecotone. *American Journal of Botany*, **88**, 919–932.

Rundel, P.W., Gordon, D.T. & Parsons, D.J. (1977) Montane and subalpine vegetation of the Sierra Nevada and Cascade Ranges. *Terrestrial vegetation of California* (ed. by M.G. Barbour and J. Major), pp. 559–600. John Wiley and Sons, New York, NY.

Running, S.W., Nemani, R.R. & Hungerford, R.D. (1987) Extrapolation of synoptic meteorological data in mountainous terrain and its use for simulating forest evapotranspiration and photosynthesis. *Canadian Journal of Forest Research*, **17**, 472–483.

Russell, C.P. (1992) *One hundred years in Yosemite*. Yosemite Association, El Portal, CA.

Stephenson, N.L. (1990) Climatic control of vegetation distribution – the role of the water balance. *The American Naturalist*, **135**, 649–670.

Stephenson, N.L. (1998) Actual evapotranspiration and deficit: biologically meaningful correlates of vegetation distribution across spatial scales. *Journal of Biogeography*, **25**, 855–870.

Stine, S. (1990) Late Holocene fluctuations of Mono Lake, eastern California. *Palaeogeography, Palaeoclimatology, Palaeoecology*, **78**, 333–381.

Stine, S. (1996) Climate, 1650–1850. *Sierra Nevada Ecosystem Project: final report to Congress, Assessments and scientific basis for management options*, pp. 25–30. Centers for Water and Wildland Resources, University of California, Davis, CA.

Sugihara, N.G., van Wagtendonk, J.W. & Fites-Kaufman, J. (2006) Fire as an ecological process. *Fire in California's ecosystems* (ed. by N.G. Sugihara, J.W. van Wagtendonk, K.E. Shaffer, J. Fites-Kaufman and A.E. Thode), pp. 58–74. University of California Press, Berkeley, CA.

Sun, G., McNulty, S.G., Lu, J., Amatya, D.M., Liang, Y. & Kolka, R.K. (2005) Regional annual water yield from forest lands and its response to potential deforestation across the southeastern United States. *Journal of Hydrology*, **308**, 258–268.

Swetnam, T.W. (1993) Fire history and climate change in giant sequoia groves. *Science*, **262**, 885–889.

Thomas, C.D., Cameron, A., Green, R.E., Bakkenes, M., Beaumont, L.J., Collingham, Y.C., Erasmus, B.F.N., de Siqueira, M.F., Grainger, A., Hannah, L., Hughes, L., Huntley, B., van Jaarsveld, A.S., Midgley, G.F., Miles, L.,

Ortega-Huerta, M.A., Peterson, A.T., Phillips, O.L. & Williams, S.E. (2004) Extinction risk from climate change. *Nature*, **427**, 145–148.

Thompson, R.S. & Anderson, K.H. (2000) Biomes of western North America at 18,000, 6000, and 0 ^{14}C yr BP reconstructed from pollen and packrat midden data. *Journal of Biogeography*, **27**, 555–584.

Thompson, R.S., Anderson, K.H. & Bartlein, P.J. (1999) *Atlas of relations between climatic parameters and distributions of important trees and shrubs in North America*. US Geological Survey Professional Paper 1650 A and B, US Geological Survey, Denver, CO.

Thompson, R.S., Anderson, K.H. & Bartlein, P.J. (2008) Quantitative estimation of bioclimatic parameters from presence/absence vegetation data in North America by the modern analog technique. *Quaternary Science Reviews*, **27**, 1234–1254.

Thorne, J.H., Morgan, B.J. & Kennedy, J.A. (2008) Vegetation change over sixty years in the central Sierra Nevada, California, USA. *Madroño*, **55**, 223–237.

Thornthwaite, C.W. (1948) An approach towards a rational classification of climate. *Geographical Review*, **38**, 55–102.

Thornthwaite, C.W. & Mather, J.R. (1955) The water balance. *Publications in Climatology*, **8**, 1–104.

Thornton, P.E., Running, S.W. & White, M.A. (1997) Generating surfaces of daily meteorological variables over large regions of complex terrain. *Journal of Hydrology*, **190**, 214–251.

Urban, D.L., Miller, C., Halpin, P.N. & Stephenson, N.L. (2000) Forest gradient response in Sierran landscapes: the physical template. *Landscape Ecology*, **15**, 603–620.

Vale, T.R. (1987) Vegetation change and park purposes in the high elevations of Yosemite National Park, California. *Annals of the Association of American Geographers*, **77**, 1–18.

Van Pelt, R. (2001) *Forest giants of the Pacific coast*. University of Washington Press, Seattle, WA.

Vankat, J.L. (1982) A gradient perspective on the vegetation of Sequoia National Park, California. *Madroño*, **29**, 200–214.

Vörösmarty, C.J., Federer, C.A. & Schloss, A.L. (1998) Evaporation functions compared on US watersheds: possible implications for global-scale water balance and terrestrial ecosystem modeling. *Journal of Hydrology*, **207**, 147–169.

van Wagtendonk, J.W. & Fites-Kaufman, J. (2006) Sierra Nevada bioregion. *Fire in California's ecosystems* (ed. by N.G. Sugihara, J.W. van Wagtendonk, K.E. Shaffer, J. Fites-Kaufman and A.E. Thode), pp. 264–294. University of California Press, Berkeley, CA.

van Wagtendonk, J.W. & Lutz, J.A. (2007) Fire regime attributes of wildland fires in Yosemite National Park, USA. *Fire Ecology*, **3(2)**, 34–52.

van Wagtendonk, J.W., van Wagtendonk, K.A., Meyer, J.B. & Painter, K.J. (2002) The use of geographic information for fire management in Yosemite National Park. *George Wright Forum*, **19**, 19–39.

Walker, R.E. (2000) *Investigations in vegetation map rectification, and the remotely sensed detection and measurement of*

natural vegetation changes. PhD Thesis, University of California Santa Barbara, Santa Barbara, CA.

Waring, R.H. & Cleary, B.D. (1967) Plant moisture stress: evaluation by pressure bomb. *Science*, **155,** 1248–1254.

Washington, W.M., Weatherly, J.W., Meehl, G.A., Semtner, A.J., Bettge, T.W., Craig, A.P., Strand, W.G., Arblaster, J., Wayland, V.B., James, R. & Zhang, Y. (2000) Parallel climate model (PCM) control and transient simulations. *Climate Dynamics*, **16,** 755–774.

Wieslander, A.E. (1935) A vegetation type map of California. *Madroño*, **3,** 140–144.

Williams, J.W. & Jackson, S.T. (2007) Novel climates, no-analog communities, and ecological surprises. *Frontiers in Ecology and the Environment*, **5,** 475–482.

Williams, J.W., Jackson, S.T. & Kutzbach, J.E. (2007) Projected distribution of novel and disappearing climates by 2100 AD. *Proceedings of the National Academy of Sciences USA*, **104,** 5738–5742.

Willmott, C.J., Rowe, C.M. & Mintz, Y. (1985) Climatology of the terrestrial seasonal water cycle. *Journal of Climatology*, **5,** 589–606.

SUPPORTING INFORMATION

Additional Supporting Information may be found in the online version of this article:

Appendix S1 Equations for calculation of annual actual evapotranspiration (AET) and annual climatic water deficit (Deficit).

As a service to our authors and readers, this journal provides supporting information supplied by the authors. Such materials are peer-reviewed and may be re-organized for online delivery, but are not copy-edited or typeset. Technical support issues arising from supporting information (other than missing files) should be addressed to the authors.

BIOSKETCHES

James A. Lutz is a post-doctoral researcher at the College of the Environment with interests in decadal- and centennial-scale vegetation change in western North America, fire ecology, and the ecophysiological basis of climate–vegetation interactions.

Jan W. van Wagtendonk is a US Geological Survey Research Forester Emeritus, whose interests include fire ecology and the ecology of the Sierra Nevada.

Jerry F. Franklin is Professor of Forestry at the University of Washington, College of the Environment. He studies western coniferous forests and takes an active role in science–policy development.

Editor: Jack Williams